helpful suggestions and discussions. Conducted in part using the ACCRE computing facility at Vanderbilt University, Nashville, TN. Supported by L. S. B. Leakey and Wenner Gren Foundation grants, NSF grants BCS-0196183, BSC-0552486, and BCS-0827436, NIH grants R01GM076637 and 1R01GM083606-01, and David and Lucile Packard and Burroughs Wellcome Foundation Career Awards (S.A.T.); NIH grant F32HG03801 (F.A.R.); and NIH grant R01 HL65234 (S.M.W. and J.H.M.). Genotyping was supported by the NHLBI Mammalian Genotyping Service. The content of this publication does not necessarily reflect the views or policies of the Department of Health and Human Services, nor does mention of trade names, commercial products, or organizations imply endorsement by the U.S. government. The project included in this manuscript has been funded in part with federal funds from the National Cancer Institute under contract N01-CO-12400. Original genotype data are available at http://research.marshfieldclinic.org/genetics/genotypingData_Statistics/humanDiversityPanel.asp. Data used for analyses in the current manuscript are available at www.med.upenn.edu/tishkoff/Supplemental/files.html and at http://chgr.mc.vanderbilt.edu/page/supplementary-data.

Supporting Online Material
www.sciencemag.org/cgi/content/full/1172257/DC1
Materials and Methods
SOM Text
Figs. S1 to S35
Tables S1 to S9
References

13 February 2009; accepted 17 April 2009
Published online 30 April 2009;
10.1126/science.1172257
Include this information when citing this paper.

REPORTS

Dispersion of the Excitations of Fractional Quantum Hall States

Igor V. Kukushkin,[1,2] Jurgen H. Smet,[1]* Vito W. Scarola,[3,4] Vladimir Umansky,[5] Klaus von Klitzing[1]

The rich correlation physics in two-dimensional (2D) electron systems is governed by the dispersion of its excitations. In the fractional quantum Hall regime, excitations involve fractionally charged quasi particles, which exhibit dispersion minima at large momenta referred to as rotons. These rotons are difficult to access with conventional techniques because of the lack of penetration depth or sample volume. Our method overcomes the limitations of conventional methods and traces the dispersion of excitations across momentum space for buried systems involving small material volume. We used surface acoustic waves, launched across the 2D system, to allow incident radiation to trigger these excitations at large momenta. Optics probed their resonant absorption. Our technique unveils the full dispersion of such excitations of several prominent correlated ground states of the 2D electron system, which has so far been inaccessible for experimentation.

In two-dimensional electron systems (2DESs) exposed to a strong perpendicular magnetic field B, interaction effects give rise to a remarkable set of quantum fluids. When all electrons reside in the lowest electronic Landau level, the kinetic energy is quenched and the Coulomb interaction then dominates. The strong repulsive interaction gives rise to the incompressible fractional quantum Hall fluids at rational fillings V_p of the lowest Landau level of the form $v_p = p/[2p \pm 1]$, $p = 1, 2, 3,\ldots$ (*1*). The appearance of these fluids may also be understood as a result of Landau quantization of a Fermi sea, which forms at filling factor $v_{p\to\infty} = 1/2$ and is composed of quasi particles referred to as composite fermions (*2*–*4*). At this filling, these composite fermions experience a vanishing effective magnetic field B_{eff}. When moving away from half filling, the composite fermions are sent into circular cyclotron orbits that they execute with frequency $\omega_{c,CF} \propto |B_{\mathrm{eff}}|$. Landau quantization of these composite fermion orbits and the successive depopulation of the associated Landau levels give rise to the incompressible fractional quantum Hall fluids. The lowest energy-neutral excitation of these fluids involves a negatively charged quasi particle with a fractional charge of $e/(2p \pm 1)$, where e is the charge on the electron (*5*–*7*), and a positively charged quasi hole that is left behind. This excitation requires an energy that, in the weakly interacting picture, corresponds to the energy gap separating adjacent composite fermion Landau levels (*4*, *8*). According to theory, these neutral excitations at fractional filling v_p possess an energy dispersion with p minima at large wave vectors q on the order of the inverse of the magnetic length $l_B = \sqrt{e/hB}$, where h is Planck's constant, or about 10^8 m^{-1} for typical densities of gallium arsenide–based 2DESs (*1*, *9*–*14*).

The minima are referred to as magneto-roton minima and are analogous to the roton minimum in the excitation dispersion that was introduced by Landau (*15*) to account for the anomalous heat capacity observed in superfluid He-II (*16*). The magneto-roton minima govern the low-

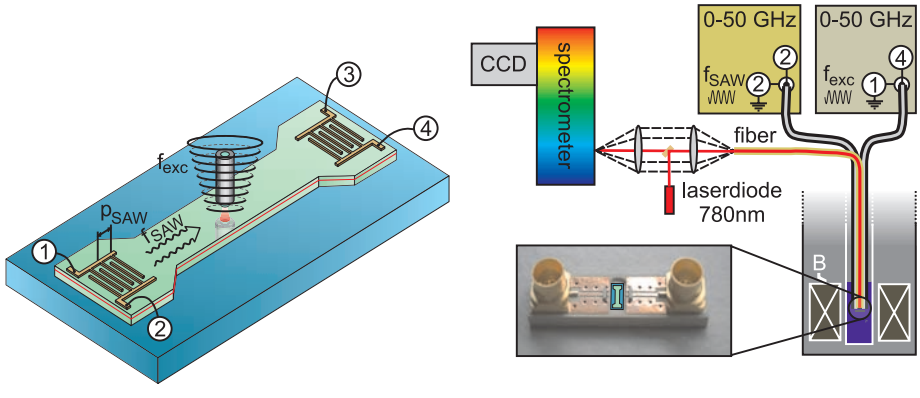

Fig. 1. Experimental arrangement for the detection of resonant microwave absorption at large wave vectors. (Left) Sample geometry consisting of a 0.1-mm-wide and 1-mm-long mesa. At its ends, the mesa widens and hosts two interdigital transducers with period p_{SAW}. High-frequency radiation drives the left transducer. The transducer launches SAWs across the sample. In the active-device region, light from a 780-nm laserdiode triggers a luminescence signal. This region of the sample is also irradiated with a quasi-monochromatic microwave by using a second high-frequency generator. Electrodes 1 and 4, which belong to transducers on opposite sides of the mesa, serve as a dipole antenna. (Right) Schematic of the cryostat configuration and the high-frequency chip carrier.

[1]Max Planck Institute for Solid State Research, D-70569 Stuttgart, Germany. [2]Institute of Solid State Physics, Russian Academy of Science, Chernogolovka 142432, Russia. [3]Department of Chemistry and Pitzer Center for Theoretical Chemistry, University of California at Berkeley, Berkeley, CA 94720, USA. [4]Theoretische Physik, Eidgenössische Technische Hochschule Zürich, 8093 Zürich, Switzerland. [5]Department of Condensed Matter Physics, Weizmann Institute of Science, Rehovot 76100, Israel.

*To whom correspondence should be addressed. E-mail: j.smet@fkf.mpg.de

temperature thermodynamic behavior and the stability of the incompressible fractional quantum Hall fluids because they are the lowest-energy excitations in the dispersion. Rotons at fillings of $p/(2p \pm 1)$ can be understood intuitively as bound states of such negatively charged quasi particles and positively charged quasi holes. These quasi particles are localized charges that move in a magnetic field on top of the p filled composite fermion Landau levels. The excitation wave functions have a nodal structure that gives rise to p oscillations in the electron pair correlation function over length scales on the order of l_B. When imparted with momentum k, the Lorentz force causes the quasi particle and hole to rotate about each other at an intercharge separation that increases with k. At large momenta ($k >> l/l_B$), the charges completely separate. But at intermediate momenta ($k \approx l/l_B$), the pair-correlation oscillations in the host liquid impose an energy gain for the charges so as to nest in one of the p correlation minima and set up a rotating bound state. The center of mass motion of the resulting p bound states, rotons, gives rise to free-particle behavior (a parabolic dispersion) for momenta near the roton minima.

Magneto-rotons in the fractional quantum Hall regime were predicted long ago (*9*–*11*), but direct experimental observation of them has remained elusive. Optical experiments would in principle only probe the excitation energy close to zero momentum. However, Kohn's theorem for a translationally invariant system implies that there is no oscillator strength in this limit. Therefore, excitations emerging from the Coulomb interaction remain invisible for small excitation wave vectors $k \rightarrow 0$ (*12*, *17*). Temperature-dependent transport addresses the opposite limit $k \rightarrow \infty$ because it requires charge separation. Powerful methods applied in other contexts, such as inelastic neutron scattering, in order to explore the regime in between both limits, has helped to confirm experimentally the roton dispersion predicted by Landau in He-II (*18*), but these methods are not useful. Inelastic neutron scattering performs very well on bulk systems, but to address a 2DES with an active region of only 10 nm is still very difficult. A surface-scattering technique such as angle-resolved photoemission spectroscopy cannot be used either because the 2DESs are buried deep underneath the crystal surface so as to obtain the highest-purity samples. Inelastic light scattering is one approach that has been applied successfully; however, control over the momentum is limited to $k < 4\pi/\lambda$ (where λ is the wavelength of the incident light). In the case of GaAs, optical excitation takes place at a wavelength of 800 nm, and the maximum momentum that can be transferred is only 1.6×10^7 m^{-1}. Roton excitations occur at larger momenta. The inevitable short-range disorder of the sample also permits inelastic light scattering to probe such large momenta; however, only extrema in the dispersion will be visible, and it is not possible to assign the observed features to a specific wave number. Even so, such studies led to the first evidence for rotons in the fractional quantum Hall regime (*19*, *20*). Also, specific heat-capacity studies that were based on the absorption of ballistic phonons have revealed signatures of magneto-rotons (*21*). Here too, the momentum dispersion remained inaccessible.

To trace the dispersion as a function of wave vector, one may impose a periodic modulation of the dielectric constant with different periodicities. Incident light is then not perceived as homogeneous by the sample, and the light can couple at the nonzero wave vector defined by the modulation. This idea has been implemented in the past in order to investigate plasmons (*22*). Similarly, inelastic light scattering studies performed at large values of k with metallic gratings were reported in the integer quantum Hall regime (*23*). However, these metallic gratings on top of the active device region are not benign. They block a large part of the incident optical radiation. The metal also screens the Coulomb interaction and modifies the physics under study.

We achieved a periodic modulation by launching surface acoustic waves (SAWs) across the 2DES. The experimental arrangement (Fig. 1) uses metallic interdigital transducers placed far away from the active device region (*24*, *25*). Three different waves are simultaneously incident on the sample: (i) A SAW propagates along the sample surface in order to impose a slowly varying modulation of the dielectric constant. The periodicity of the interdigital transducer p_{SAW} fixes the SAW wavelength at $\lambda_{SAW} = p_{SAW}$ and the resonance frequency at $f_{SAW} = v_{sound}/\lambda_{SAW}$, where v_{sound} is the velocity of sound in GaAs (approximately 2850 m s^{-1}). The modulation period λ_{SAW} defines the momentum k_{SAW} at which the excitations are probed. We repeated the experiments

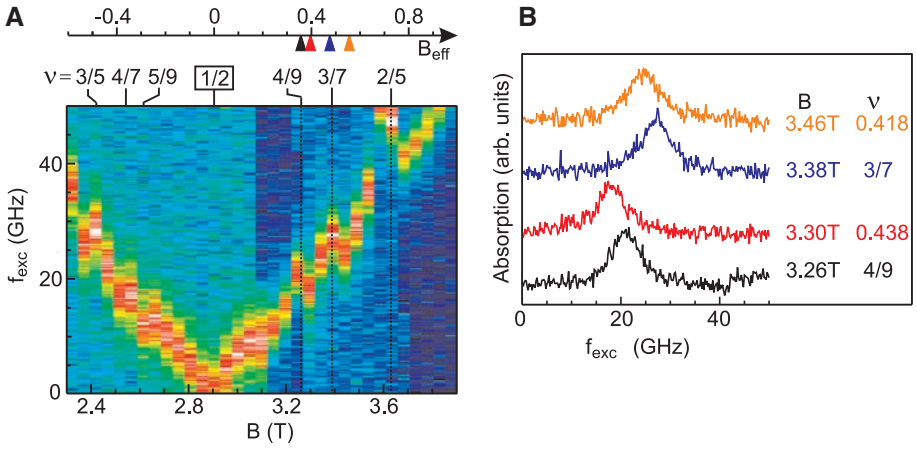

Fig. 2. The absorption of microwave radiation with frequency f_{exc} in the vicinity of filling factor 1/2 as a function of the magnetic field B for $k_{SAW} = 3.9 \times 10^5$ cm^{-1} ($f_{SAW} = 18$ GHz) and a carrier density of 3.5×10^{10} cm^{-2}. (**A**) Color rendition of the absorption strength as a function of the magnetic field and the incident microwave radiation f_{exc}. Blue colors correspond to weak absorption. Absorption maxima appear in red. The differential luminescence spectra were recorded at 30 mK. Prominent fractional states are marked at the top. (**B**) Vertical cuts through the data of (A) for filling factors smaller than 1/2. The absorption peak does not monotonically shift to a higher frequency with an increase of the effective magnetic field.

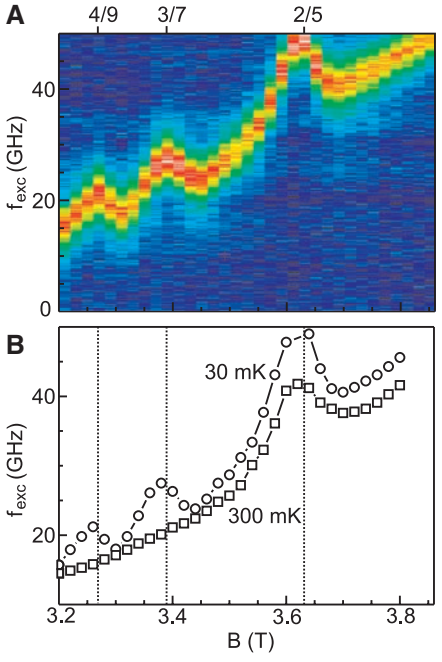

Fig. 3. The absorption strength of microwave radiation with frequency f_{exc} recorded with higher resolution as a function of the magnetic field B for $k_{SAW} = 3.9 \times 10^5$ cm^{-1} ($f_{SAW} = 18$ GHz) and a density of 3.5×10^{10} cm^{-2}. (**A**) Color rendition of the absorption strength in the magnetic field versus the frequency plane. Blue colors correspond to weak absorption. Absorption maxima appear in red. The resonance frequency oscillates with the magnetic field and reaches maxima at prominent fractional filling factors. (**B**) The resonant absorption frequency as a function of the applied magnetic field for two different temperatures, 30 and 300 mK.

for transducers with different periodicities down to 120 nm (24 GHz). By driving these transducers in a contactless fashion at double the frequency in order to preferentially excite their second harmonic (*24*), it is possible to cover momenta up to 10.4×10^8 m^{-1}. (ii) A second high-frequency generator irradiates the active-device region with a wave at frequency f_{exc}. When the photon energy hf_{exc} matches the energy of an excitation at wave vector k_{SAW} of the 2DES, resonant absorption may occur. Resonant absorption heats up the system and causes a thermal redistribution of charge carriers. (iii) Incident laser light at a wavelength of 780 nm triggers luminescence. Its spectrum is sensitive to the thermal distribution of the charge carriers. By comparing the luminescence in the absence and presence of the microwave radiation f_{exc}, we built the differential spectrum so as to reveal the resonant absorption profile. The integral of the absolute value of the differential spectrum across the recorded spectral range serves as a measure of the absorption strength.

This technique (and its derivatives) can also be applied to detect the electron-spin resonance and the composite fermion cyclotron resonance mode at a large nonzero wave vector (*26*, *27*). Studies on the well-known magnetoplasmon excitations at moderate magnetic fields have confirmed that with this technique, excitations are triggered at a wave vector with magnitude k_{SAW}. A typical example of such investigations has been included as supporting online material (SOM) text. The influence of the SAW seems to be limited to aiding the transfer of momentum. Apparently, no absorption of the SAW phonon takes place, as is demonstrated in the SOM for the electron-spin resonance (SOM text). Figure 2 plots an example of the microwave absorption strength as a function of the applied magnetic field and the incident microwave frequency f_{exc} at large magnetic fields around filling factor 1/2. Figure 2A displays a color rendition covering the magnetic field and frequency parameter space, and Fig. 2B highlights selected line scans at fixed values of the magnetic field. At low values of the effective magnetic field, two resonances or maxima in the absorption strength appear for each frequency f_{exc}. They are symmetrically arranged around filling factor 1/2. They have a width of ~10 GHz or less (which corresponds to 40 μeV) and can be attributed to the cyclotron resonance of composite fermions at the nonzero wave vector defined by the SAW (*26*). The frequency drops approximately linearly to zero as these resonances approach filling factor 1/2. It reflects the linear dependence of the composite fermion cyclotron frequency $\omega_{c,CF}$ on the effective magnetic field.

Further away from filling factor 1/2, however, deviations from a linear dependence are apparent in Fig. 2A. The resonance frequency starts to oscillate as the effective magnetic field increases. Some prominent fractional fillings have been marked in Fig. 2A and reveal that the largest deviations from a linear dependence occur at fields in which the 2DES is expected to condense into a fractional quantum Hall fluid. Figure 3A depicts a smaller region of the (B, f_{exc})–parameter space. It has been recorded with longer accumulation times and with a smaller magnetic field step size in order to better bring out the oscillatory features. For the parameters of the experiment, the maxima at fillings 2/5, 3/7, and 4/9 are the optical signatures for the formation of an incompressible fractional quantum Hall state that can be interpreted as an integer quantum Hall state of composite fermions. The resonance frequency yields the energy gap, which is the energy cost required to create a neutral quasi particle–quasi hole excitation at momentum k_{SAW}. The strongest fractional filling factor, 1/3, is out of reach because the energy gap exceeds the maximum accessible frequency f_{exc} of 50 GHz.

We emphasize that the oscillatory features in the absorption due to the correlation-driven condensation of composite fermions in incompressible states are only observable at the lowest temperatures. These features vanish for the 4/9 and 3/7 fractional quantum Hall states upon increasing the temperature (T) to 300 mK, whereas the feature is strongly reduced for the 2/5 state. This temperature-dependent behavior is illustrated in Fig. 3B. Even though the increase in T to 300 mK destroyed the formation of the more fragile fractional quantum Hall states, the composite particles themselves survive because at the cyclotron resonance frequency, resonant absorption can be observed up to considerably higher temperatures. Further temperature-dependent features of the resonances are deferred to the SOM text.

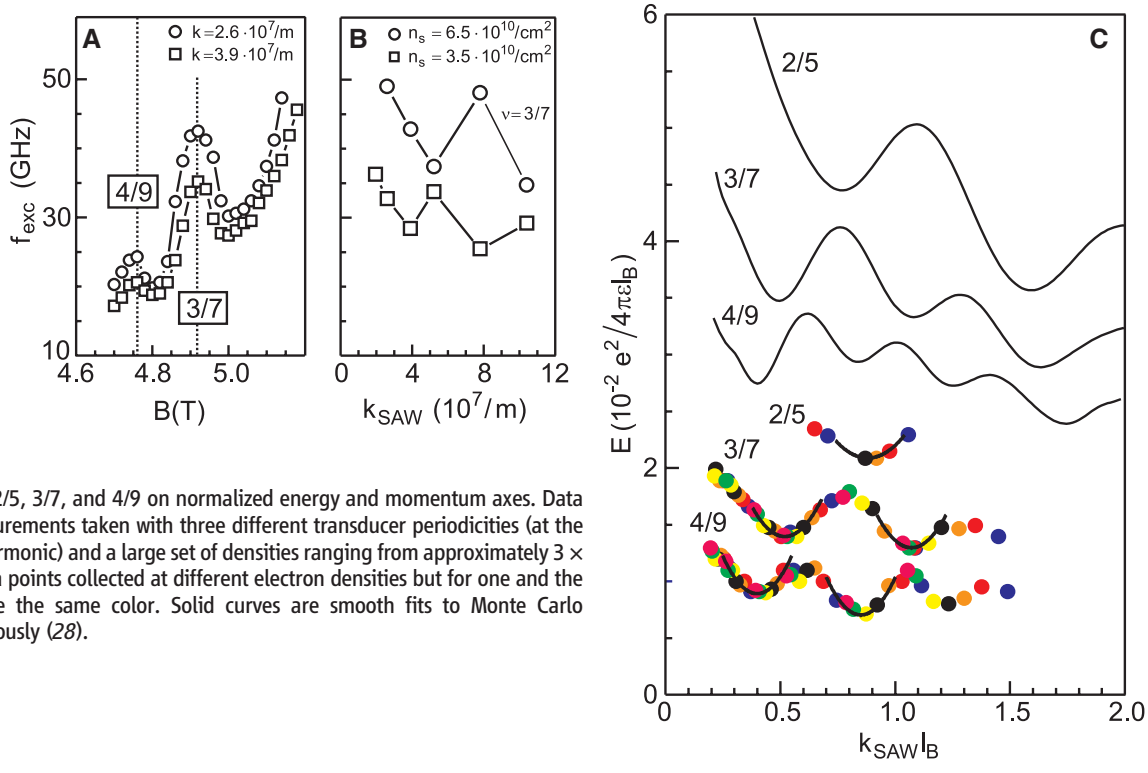

Fig. 4. Roton dispersion at filling factors 2/5, 3/7, and 4/9. (**A**) Resonant absorption frequency as a function of the applied magnetic field for two different momentum values $k_{SAW} = 2.6 \times 10^7$ m^{-1} and 3.9×10^7 m^{-1} at an electron density of 5.1×10^{10} cm^{-2} and a temperature of 30 mK. (**B**) Resonance frequency at filling factor 3/7 as a function of momentum k_{SAW} for two different values of the carrier density. (**C**) Dispersion of the resonance frequency at filling factors 2/5, 3/7, and 4/9 on normalized energy and momentum axes. Data points originate from measurements taken with three different transducer periodicities (at the fundamental and second harmonic) and a large set of densities ranging from approximately 3×10^{10} to 7×10^{10} cm^{-2}. Data points collected at different electron densities but for one and the same k_{SAW} transducer have the same color. Solid curves are smooth fits to Monte Carlo simulations described previously (*28*).

The oscillatory features were observed at all investigated values of the electron density as well as for the different momentum values k_{SAW} supplied by the SAW transducers. Example traces in Fig. 4A depict the magnetic field–dependence of the resonant microwave frequency for two different values of k_{SAW} (2.6×10^7 m^{-1} and 3.9×10^7 m^{-1}) and a density of 5.1×10^{10} cm^{-2} and $T = 30$ mK. Evidently, the energy gaps of the incompressible states substantially depend on the transferred momentum k_{SAW}. Figure 4B plots the resonant frequency at fractional filling 3/7 for the different values of k_{SAW} covered by the fabricated set of transducers (p_{SAW} = 120, 160, and 240 nm and contactless excitation of the second harmonic). Data sets are shown for two electron densities: 3.5×10^{10} cm^{-2} and 6.5×10^{10} cm^2. Despite the limited number of data points, the dispersion of the gap excitation at filling 3/7 is clearly a nonmonotonic function of k_{SAW}. Several minima are present, indicating that residual quasi particle–quasi hole correlations modify the absorption frequency. We assigned these minima to roton minima in the quasi particle dispersion. Varying the electron density influences the position of these minima. In order to compose a curve with more data points, the same experiment was repeated at several carrier densities. The circles in Fig. 4C display our primary results, the measured dispersions for the fractional states at filling factors 2/5, 3/7, and 4/9. These traces were compiled from data points taken at electron densities between 3×10^{10} and 7×10^{10} cm^{-2}. The energy is plotted in units of the Coulomb interaction strength $E_C = e^2/4\pi\varepsilon l_B$, the relevant energy scale in the lowest Landau level. Here, e is the electron charge and ε is the permittivity of GaAs. Usually, density-induced changes in the width of the electron wave function introduce complications for such a normalization procedure. However, in the investigated range of densities, the interparticle separation is considerably larger than the width of the electron wave function, and the form factor remains close to 1 (*28*). According to theory, the gap excitations of fractional quantum Hall states possess a parabolic dispersion near the roton minimum wave vector k_{roton}. For fractional fillings of the form $p/(2p + 1)$, a total of p minima is expected. In the accessible range of momenta, a single roton-like minimum is observed for the fractional quantum Hall state at filling 2/5, two minima are distinguishable for the 3/7 state, and three minima appear for the 4/9 state. We are unable to reach the last minimum for each of these fractional quantum Hall states because the required momentum transfer exceeds our present capabilities. The SOM text illustrates how the dispersion at fractional filling 3/7 changes with temperature and as one moves away from the quantized Hall state. At 300 mK, the roton features largely vanish. They also disappear at filling factors at which the system does not condense in a fractional quantum Hall state.

In the vicinity of each minimum, the dispersion is described well by a parabola, $E(k)/E_C = E_{roton}/E_C + \frac{\hbar^2(kl_B - k_{roton}l_B)^2}{2l_B^2 E_C m_{roton}}$, as illustrated by the solid black lines in Fig. 4C. Here, E_{roton} is the gap energy at the minimum and m_{roton} is referred to as the roton mass. Minima belonging to one and the same fractional quantum Hall state are fitted well, assuming the same roton mass. Table S1 in the supporting material lists the experimentally determined normalized values of E_{roton}, k_{roton}, and the inverse roton mass $1/m_{roton}$ for each minimum.

We compared our experimentally determined dispersion with the dispersion obtained from the composite fermion wave functions (*28*). These calculations are included as solid lines in Fig. 4C. They are smooth fits through Monte Carlo simulation data with typical uncertainties of $\leq 0.002E_C$. The simulations have no fitting parameters and take into account the finite thickness of the 30-nm-wide square quantum well at a density of 7×10^{10} cm^{-2}. The right panel of Table S1 shows roton parameters of the theoretical dispersion curves extracted by using a nonlinear least-square parabolic fit to the Monte Carlo data near the roton minima. The positions of the roton minima match well with the experimentally obtained values. For the 2/5 state, the deviation from the theoretical estimate of the roton mass falls within the experimental accuracy. However, the energy E_{roton} is systematically smaller in experiment by roughly a factor of 2 for the well-developed 2/5 and 3/7 fractional quantum Hall states. Because the nonzero width of the wave function was included, disorder broadening as well as Landau-level mixing are the remaining suspects for this discrepancy between theory and experiment. Landau-level mixing may cause a deviation on the order of 10% but not 100%. Hence, disorder, not included in existing theory, is probably responsible for the substantial reduction of the gap.

The fractional quantum Hall effect ground states are uniform liquids, whereas excitations lead to spatial oscillations in charge density over distances on the order of the magnetic length l_B. Charge disorder will couple to excited states more strongly than to a uniform state, lowering the energy difference between these two states; that is, disorder lowers the gap. If disorder perturbs the 2DES on length scales much longer than the magnetic length, then this just results in an overall energy shift. If disorder perturbs the 2DES on shorter length scales, we would expect a k-dependent distortion of the roton dispersion and therefore altered effective masses. The agreement between theory and experiment in comparison of the roton masses and the position of the minima suggests that disorder length scales are much larger than the magnetic length. Because the magnetic length is on the order of 10 nm, this is plausible for these high-quality structures. Also, a nearby conducting plane may strongly affect the energy gap. Such a parallel layer may indeed exist in the doped region of the heterostructure because of the optical excitation during the experiment. Here, this layer is located at a distance of 80 nm from the 2DES. Image charges would screen the Coulomb interaction and lower the gap.

References and Notes

1. R. E. Prange, S. M. Girvin, Eds., *The Quantum Hall Effect* (Springer, New York, 1990).
2. J. K. Jain, *Phys. Rev. Lett.* **63**, 199 (1989).
3. B. I. Halperin, P. A. Lee, N. Read, *Phys. Rev. B* **47**, 7312 (1993).
4. O. Heinonen, Ed., *Composite Fermions: A Unified View of the Quantum Hall Regime* (World Scientific Publishing Company, Singapore, 1998).
5. R. B. Laughlin, *Phys. Rev. Lett.* **50**, 1395 (1983).
6. R. de-Picciotto *et al.*, *Nature* **389**, 162 (1997).
7. L. Saminadayar, D. C. Glattli, Y. Jin, B. Etienne, *Phys. Rev. Lett.* **79**, 2526 (1997).
8. B. I. Halperin, P. A. Lee, N. Read, *Phys. Rev. B* **47**, 7312 (1993).
9. C. Kallin, B. I. Halperin, *Phys. Rev. B* **30**, 5655 (1984).
10. F. D. M. Haldane, E. H. Rezayi, *Phys. Rev. Lett.* **54**, 237 (1985).
11. S. M. Girvin, A. H. MacDonald, P. M. Platzman, *Phys. Rev. Lett.* **54**, 581 (1985).
12. S. M. Girvin, A. H. MacDonald, P. M. Platzman, *Phys. Rev. B* **33**, 2481 (1986).
13. M. Rasolt, A. H. MacDonald, *Phys. Rev. B* **34**, 5530 (1986).
14. S. H. Simon, B. I. Halperin, *Phys. Rev. B* **48**, 17368 (1993).
15. L. Landau, *Phys. Rev.* **60**, 356 (1941).
16. P. L. Kapitza, *Phys. Rev.* **60**, 354 (1941).
17. W. Kohn, *Phys. Rev.* **123**, 1242 (1961).
18. J. L. Yarnell, G. P. Arnold, P. J. Bendt, E. C. Kerr, *Phys. Rev.* **113**, 1379 (1959).
19. A. Pinczuk, B. Denis, L. N. Pfeiffer, K. West, *Phys. Rev. Lett.* **70**, 3983 (1993).
20. A. Pinczuk *et al.*, *Am. Phys. Soc.* **40**, 515 (1995).
21. U. Zeitler *et al.*, *Phys. Rev. Lett.* **82**, 5333 (1999).
22. E. Batke, D. Heitmann, J. P. Kotthaus, K. Ploog, *Phys. Rev. Lett.* **54**, 2367 (1985).
23. L. L. Sohn *et al.*, *Solid State Commun.* **93**, 897 (1995).
24. I. V. Kukushkin *et al.*, *Appl. Phys. Lett.* **85**, 4526 (2004).
25. Materials and methods are available as supporting material on *Science* Online.
26. I. V. Kukushkin *et al.*, *Phys. Rev. Lett.* **96**, 126807 (2006).
27. I. V. Kukushkin *et al.*, *Phys. Rev. Lett.* **98**, 066403 (2007).
28. V. W. Scarola, K. Park, J. K. Jain, *Phys. Rev. B* **61**, 13064 (2000).

29. We acknowledge financial support from the Deutsche Forschungsgemeinschaft, the German Israeli Foundation, and the Bundesministerium für Bildung und Forschung.

Supporting Online Material

www.sciencemag.org/cgi/content/full/1171472/DC1
Materials and Methods
SOM Text
Figs. S1 to S4
Table S1
References

27 January 2009; accepted 3 April 2009
Published online 30 April 2009;
10.1126/science.1171472
Include this information when citing this paper.

Dispersion of the Excitations of Fractional Quantum Hall States

Igor V. Kukushkin, Jurgen H. Smet, Vito W. Scarola, Vladimir Umansky and Klaus von Klitzing

Science **324** (5930), 1044-1047.
DOI: 10.1126/science.1171472originally published online April 30, 2009

Getting Below the Surface

Two-dimensional electron systems have proved to be a productive area for the study of low-dimensional transport. Despite decades of intense effort, the actual dispersion of the electronic excitations—how their energy behaves as a function of momentum as the they move through their two-dimensional space—have eluded experiments. This elusiveness is due to the samples being thin and buried. **Kukushkin *et al.*** (p. 1044; published online 30 April; see the Perspective by **Simon**) now introduce a technique based on launching surface acoustic waves through the sample. The excitations "ride" these waves, with their energy and momentum mapped out using pulses of laser light. The technique should also be applicable to other hard-to-get-at electronic systems.